International Symposium
On Turbulence and Shear Flow
Phenomena (TSFP-9)
June 30 - July 3, 2015 *Melbourne, Australia*

IMPLICIT DIRECT FORCING FOR LOW REYNOLDS NUMBER FLOWS

Hyunwook Park
Department of Computational Science
and Engineering, Yonsei University
Seoul 120-749
deukyun@naver.com

Changhoon Lee
Department of Computational Science
and Engineering, Yonsei University
Seoul 120-749
clee@yonsei.ac.kr

Jung-Il Choi
Department of Computational Science
and Engineering, Yonsei University
Seoul 120-749
jic@yonsei.ac.kr

ABSTRACT

A novel immersed boundary (IB) method based on an implicit direct forcing (IDF) scheme is developed for incompressible viscous flows. A key idea for the present IDF method is to use block LU decomposition technique in momentum equations and Taylor series expansion in order to construct IB forcing in a recurrence form, which leads to impose more accurate no-slip boundary conditions on the IB surface. To accelerate a convergence of the IB forcing during an iterative procedure, the pre-conditioning parameter is introduced in the formulation of the recurrence form. We perform numerical simulations of two-dimensional flows around a circular cylinder for low and moderate Reynolds numbers. The result shows that the present IDF yields a better imposition of no-slip boundary conditions on the IB surfaces for low Reynolds number with a fairly larger time step than IB methods with different direct forcing schemes due to an implicit treatment of diffusion term for determining the IB forcing.

Introduction

The immersed boundary (IB) method was firstly developed by Peskin to model flow around a flexible heart (Peskin, 1977). In IB method, the simulation is implemented on the fixed Cartesian grid, and the boundary condition at the surface of the object is indirectly imposed by adding a continuous IB forcing at the neighboring points of the object surface. The continuous IB forcing approach has been known to be appropriate to resolve fluid-flexible body interactions. However, this approach suffers from a numerical instability due to the extremely large stiffness parameter for mimicking a rigid body.

On the other hand, Fadlun *et al.* (2000) proposed a discrete forcing approach for describing an immersed rigid body in flow fields, where the IB forcing is given as a source term in momentum equation. Later, Uhlmann (2005) developed an IB method with direct forcing (DF) scheme for imposing no-slip boundary conditions on IB surface. The IB method with DF scheme has been widely used in many applications involving fluid-solid interaction problems because of the simplicity in its implementation. However, the method may less accurately impose the boundary condition on the IB surface, because the IB forcing is explicitly calculated by neglecting viscous term. To improve numerical accuracy, the multi-direct forcing (MDF) methods were introduced as an extension of DF method (Wang *et al.*, 2008; Kempe & Fröhlich, 2012), where both of the IB forcing and the provisional velocity are iteratively calculated. Although the MDF schemes enable to more accurately impose the boundary conditions at the IB surface than DF scheme, velocity errors at the IB surface may not be negligible for low Reynolds number flows.

This paper focuses on developing a novel immersed boundary method based on implicit direct forcing (IDF) scheme in order to impose more accurate no-slip boundary condition on the IB surface. We use a block LU decomposition technique for the system matrix and Taylor series expansion for obtaining a recurrence formula of the IB forcing. For an efficient computation, a pre-conditioning technique is also applied to the recurrence formula. Theoretical and numerical comparisons of other direct forcing schemes (Uhlmann, 2005; Kempe & Fröhlich, 2012) show that the present IDF scheme is more accurate in imposing the no-slip boundary conditions on the IB surface. Details of numerical simulation results will be presented at the meeting.

Immersed boundary method

Projection method

The Navier-Stokes equations for incompressible flows are written as,

$$\frac{\partial \mathbf{u}}{\partial t} + \mathbf{u}\cdot\nabla\mathbf{u} = -\nabla p + \frac{1}{Re}\nabla^2\mathbf{u} + \mathbf{f}, \tag{1}$$

$$\nabla\cdot\mathbf{u} = 0, \tag{2}$$

where $\mathbf{u}, p, Re$, and $\mathbf{f}$ are the non-dimensionalized velocity vector, pressure, Reynolds number, and volume forcing, re-

spectively. These equations are discretized in a staggered grid with finite difference formulations using the implicit Crank-Nicolson(CN) time integration for both of the viscous terms and convective terms. The numerical procedures based on the velocity-components decoupled projection method (Kim *et al.*, 2002) in matrix-vector forms are summarized as,

$$\mathscr{A}\mathbf{u}^* - \mathbf{f} = \mathbf{r}, \tag{3}$$

$$\Delta t\ \mathscr{D}\mathscr{G}\delta p = \mathscr{D}\mathbf{u}^*, \tag{4}$$

$$\mathbf{u^{n+1}} = \mathbf{u}^* - \Delta t\ \mathscr{G}\delta p, \tag{5}$$

$$p^{n+1/2} = p^{n-1/2} + \delta p, \tag{6}$$

where a system matrix $\mathscr{A}$ and residual vector $\mathbf{r}$ are defined as

$$\mathscr{A} = \frac{1}{\Delta t}\left[I + \Delta t\left(\mathscr{N} - \frac{1}{2Re}\mathscr{L}\right)\right], \tag{7}$$

$$\mathbf{r} = \frac{1}{\Delta t}u^n - \mathscr{G}p^{n-1/2} + \frac{1}{2Re}\mathscr{L}\mathbf{u}^n. \tag{8}$$

Here, $\mathbf{u}^*$ is an intermediate velocity vector and δp is a pressure difference. Discrete operators $\mathscr{L}, \mathscr{N}, \mathscr{G}$ and $\mathscr{D}$ represent the discrete Laplacian viscous operator, convective operator, gradient operator and divergence operator, respectively. The discrete operators are evaluated using the second-order central difference scheme on the staggered grid. Here, Δt is the time increment and the superscript n denotes the n^{th} time step. For the operator $\mathscr{N}$, the nonlinear terms are linearized by fully decoupling procedure (Kim *et al.*, 2002). The system matrix $\mathscr{A}$ is approximately factorized in solving Eq.(3), which enables to use a tridiagonal matrix solver with preserving second order accuracy in time. The Poisson equation in Eq.(4) is solved using a multi-grid method. In Eq.(3), $\mathbf{f}$ is the forcing which imposes the no-slip condition at immersed surfaces. Note that the forcing is kept in the left hand side of Eq.(3). The reason for the forcing being left side in that equation is to implicitly determine the forcing. Details for the implicit treatment of the forcing are discussed in the next section.

Immersed boundary method with implicit direct forcing

System matrix The present immersed boundary method uses two kinds of grids for a computational domain (Ω) as shown in Figure 1. One is the Eulerian grid where the Navier-Stokes equation is computed. The Eulerian grid nodes ($\mathbf{x}_E \in \Omega$) are uniformly distributed with a grid spacing h. The other one is the Lagrangian grid which exactly represents a set of Lagrangian points ($\mathbf{X}_L \in \Gamma$) on the IB surface. The velocity at a Lagrangian point can be interpolated using the velocity distributions on the Eulerian grid as follows:

$$\mathbf{U}(\mathbf{X}_L) = \sum_E \mathbf{u}(\mathbf{x}_E)\delta_h(\mathbf{x}_E - \mathbf{X}_L)h^3 \tag{9}$$

where $\mathbf{U}(\mathbf{X}_L)$ is the velocity at the Lagrangian point $\mathbf{X}_L$ while $\mathbf{x}_E$ represents a point in the Eulerian grid and $\mathbf{u}(\mathbf{x}_E)$ is the velocity at the point. The discrete delta function (δ_h) in Roma *et al.* (1999) is used for the interpolation:

$$\delta_h(\mathbf{x}) = \frac{1}{h^3}\phi\left(\frac{x}{h}\right)\phi\left(\frac{y}{h}\right)\phi\left(\frac{z}{h}\right) \tag{10}$$

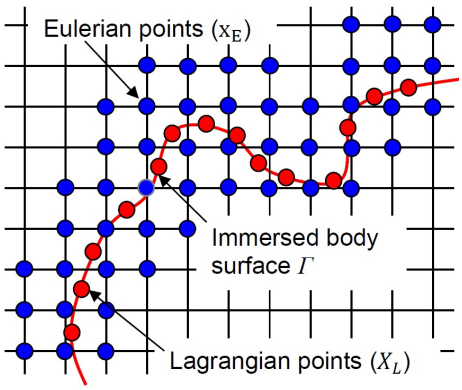

Figure 1. Lagrangian and Eulerian grid points in a computational domain (Ω).

where x, y, and z are the Cartesian coordinates and ϕ is a continuous function that is defined as

$$\phi(r) = \begin{cases} \frac{1}{6}\left(5 - 3|r| - \sqrt{1 - 3(1-|r|)^2}\right), & 0.5 \le |r| \le 1.5, \\ \frac{1}{3}\left(1 + \sqrt{-3r^2 + 1}\right), & |r| \le 0.5, \\ 0, & \text{otherwise.} \end{cases} \tag{11}$$

Using Eq. (9), the velocity at the Lagrangian points holds on $\mathbf{U} = \mathscr{B}_I\mathbf{u}$, where $\mathbf{U}$ is the velocity vector at the Lagrangian points and $\mathscr{B}_I$ is interpolation operator matrix which has $N_L \times N_E$ dimension where N_L and N_E are total number of the Lagrangian and Eulerian points, respectively. The elements for $\mathscr{B}_I$ are defined as $(\mathscr{B}_I)_{ij} = \delta_h(x_i - X_j)h^3$, where the subscripts i and j refer to a column and row of $\mathscr{B}_I$ operator matrix, respectively. Similarly, the immersed boundary forcing $\mathbf{F}$ at the Lagrangian points are extrapolated to the equivalent volume forcing $\mathbf{f}$ at the Eulerian points by $\mathbf{f} = B_E\mathbf{F}$, where $\mathscr{B}_E$ is the extrapolation operator matrix which has $N_E \times N_L$ dimension. Its elements are given as $(\mathscr{B}_E)_{ji} = \delta_h(x_i - X_j)\triangle V_L$, where $\triangle V_L$ is the discrete volume at the Lagrangian grid. Here, we assume that the discrete volume at the Lagrangian grid is the same as the discrete volume at the Eulerian grid ($\triangle V_L = h^3$). The transpose of the interpolation operator matrix is equal to the extrapolation operator matrix: $\mathscr{B}_I = (\mathscr{B}_E)^T$.

We propose an implicit direct forcing (IDF) scheme for the IB method that applies the no-slip condition to the intermediate velocity $\mathbf{u}^*$ in order to avoid no additional Poisson-type pressure solution procedure. The basic formulation of the present method from Eqs.(3) and (14), and the no-slip boundary condition at the IB surface can be written as,

$$\mathscr{A}\mathbf{u}^* - \mathscr{B}_E\mathbf{F} = \mathbf{r}, \tag{12}$$

$$\mathscr{B}_I\mathbf{u}^* = \mathbf{U_d}, \tag{13}$$

where $\mathbf{U_d}$ and $\mathbf{F}$ are the desired velocity and forcing at the IB surface, respectively. Note that Eq. (13) is a constraint for velocity field near the IB surface related to the no-slip boundary condition. A monolithic formulation for Eqs. (12) and (13) in matrix form is following as,

$$\begin{pmatrix} \mathscr{A} & -\mathscr{B}_E \\ \mathscr{B}_I & 0 \end{pmatrix}\begin{pmatrix} \mathbf{u}^* \\ \mathbf{F} \end{pmatrix} = \begin{pmatrix} \mathbf{r} \\ \mathbf{U_d} \end{pmatrix}. \tag{14}$$

By applying a block LU decomposition, Eq. (14) can be split into the following three-step procedure:

$$\mathscr{A}\mathbf{u}^{*,0} = \mathbf{r} \tag{15}$$

$$\mathscr{B}_I\mathscr{A}^{-1}\mathscr{B}_E\mathbf{F} = \mathbf{U_d} - \mathscr{B}_I\mathbf{u}^{*,0} \tag{16}$$

$$\mathbf{u}^* = \mathbf{u}^{*,0} + \mathscr{A}^{-1}\mathscr{B}_E\mathbf{F} \tag{17}$$

Without a loss of accuracy, $\mathbf{u}^*$ and $\mathbf{F}$ can be obtained from the decoupled procedure in Eqs.(15)-(17). A new intermediate velocity $\mathbf{u}^{*,0}$ is calculated from the momentum equation without volume forcing in Eq.(15). Then, solving Eq. (16) with the known $\mathbf{u}^{*,0}$ determines $\mathbf{F}$ that imposes the no-slip condition on the Lagrangian points. The intermediate velocity $\mathbf{u}^*$ can be obtained from Eq.(17) with the already determined $\mathbf{F}$. Since a direct calculation of the inverse of $\mathscr{A}$ is difficult due to an intensive computation and huge storage, $\mathbf{u}^*$ can be obtained from solving a linear equation resulted from multiplying $\mathscr{A}$ to Eq.(17) as follows:

$$\mathscr{A}\mathbf{u}^* = \mathscr{B}_E\mathbf{F} + \mathscr{A}\mathbf{u}^{*,0} = \mathscr{B}_E\mathbf{F} + \mathbf{r} \tag{18}$$

Iterative procedure Due to a huge computational complexity ($O(N_L^2N_E^4)$) for the matrix multiplication in $\mathscr{B}_I\mathscr{A}^{-1}\mathscr{B}_E$, a direct or iterative solution procedure for Eq.(16) may not be appropriate to obtain the IB forcing $\mathbf{F}$. We propose an approximate inverse procedure of $\mathscr{B}_I\mathscr{A}^{-1}\mathscr{B}_E$ using Taylor series expansion. To avoid a limitation in the use of Taylor series expansion, we introduce a $N_L \times N_L$ pre-conditioner matrix $\mathscr{P}$ assuming that $\mathscr{P}(\mathscr{B}_I\mathscr{A}^{-1}\mathscr{B}_E)$ is invertible and $\|\mathscr{P}(\mathscr{B}_I\mathscr{A}^{-1}\mathscr{B}_E)\| \leq 1$. Note that $\|\ \|$ indicates bf a matrix norm. Multiplying $\left[\mathscr{P}(\mathscr{B}_I\mathscr{A}^{-1}\mathscr{B}_E)\right]^{-1}\mathscr{P}$ to the both sides of Eq.(16) yields to

$$\mathbf{F} = \left[\mathscr{P}(\mathscr{B}_I\mathscr{A}^{-1}\mathscr{B}_E)\right]^{-1}\mathscr{P}(\mathbf{U_d} - \mathscr{B}_I\mathbf{u}^{*,0}). \tag{19}$$

By applying a truncated Taylor series expansion to Eq.(19), an approximate forcing $\mathbf{F}^k$ with order of k in a recurrence form can be expressed as

$$\mathbf{F}^k = \left[\mathscr{I}_{N_L} - \mathscr{P}(\mathscr{B}_I\mathscr{A}^{-1}\mathscr{B}_E)\right]\mathbf{F}^{k-1} + \mathscr{P}(\mathbf{U_d} - \mathscr{B}_I\mathbf{u}^{*,0}). \tag{20}$$

Assuming $\mathbf{F}^0 = \mathbf{0}$, the increment of the truncated forcing in successive truncation orders can be determined by

$$\begin{aligned}\triangle\mathbf{F} &\equiv \mathbf{F}^k - \mathbf{F}^{k-1} \\ &= \mathscr{P}(\mathbf{U_d} - \mathscr{B}_I\mathbf{u}^{*,0}) - \mathscr{P}(\mathscr{B}_I\mathscr{A}^{-1}\mathscr{B}_E)\mathbf{F}^{k-1} \\ &= \mathscr{P}\mathbf{U_d} - \mathscr{P}\mathscr{B}_I(\mathscr{A}^{-1}\mathscr{B}_E\mathbf{F}^{k-1} + \mathbf{u}^{*,0}) \\ &= \mathscr{P}(\mathbf{U_d} - \mathscr{B}_I\mathbf{u}^{*,k-1}),\end{aligned} \tag{21}$$

where an truncated velocity $\mathbf{u}^{*,k-1}$ at the order of $k-1$ can be obtained from Eq. (17) with $\mathbf{F} = \mathbf{F}^{k-1}$. The solution procedure for the present IDF is summarized as

$$\mathbf{F}^k = \mathbf{F}^{k-1} + \mathscr{P}\left(\mathbf{U_d} - \mathscr{B}_I\mathbf{u}^{*,k-1}\right), \tag{22}$$

$$\mathscr{A}\mathbf{u}^{*,k} = \mathscr{B}_E\mathbf{F}^k + \mathbf{r}, \tag{23}$$

where the order k can be interpreted as an iteration number for the IDF.

Choice of pre-conditioner The role of the pre-conditioner matrix $\mathscr{P}$ is to decrease the magnitude and condition number of the matrix $\mathscr{B}_I\mathscr{A}^{-1}\mathscr{B}_E$ in Eq. (19) for an efficient iterative procedure in Eqs. (22) and (23). Although the ideal choice of $\mathscr{P}$ is to use the inverse matrix of $\mathscr{B}_I\mathscr{A}^{-1}\mathscr{B}_E$, which is not feasible due to a heavy computational cost for calculating $\mathscr{A}^{-1}$. To overcome this issue, we consider an approximate procedure of the inverse matrix $\mathscr{A}^{-1}$ for constructing a pre-conditioner matrix $\mathscr{P}$. First, we define an appropriate pre-conditioner matrix as $\mathscr{P} = (\mathscr{B}_I\mathscr{A}_{\mathscr{P}}^{-1}\mathscr{B}_E)^{-1}$ by ignoring the convection term in $\mathscr{A}$ for simplicity. The corresponding $\mathscr{A}_{\mathscr{P}}$ is given as,

$$\mathscr{A}_{\mathscr{P}} = \frac{1}{\triangle t}\left(I - \frac{\triangle t}{2Re}\mathscr{L}\right). \tag{24}$$

The inverse of $\mathscr{A}_{\mathscr{P}}$ matrix in Eq. (24) can be approximated by using Taylor series expansion for the two limiting cases. For $\|\triangle t/(2Re)\mathscr{L}\| \ll 1$ with a second-order temporal accuracy, the inverse of $\mathscr{A}_{\mathscr{P}}$ matrix is expressed as,

$$\mathscr{A}_{\mathscr{P}}^{-1} \approx \triangle t\mathscr{I}_{N_E}, \tag{25}$$

which implies the case with a sufficiently small $\triangle t$ or high Reynolds number. Therefore, the pre-conditioner $\mathscr{P}$ can be defined as,

$$\mathscr{P} = \left(\mathscr{B}_I\mathscr{A}_{\mathscr{P}}^{-1}\mathscr{B}_E\right)^{-1} = \frac{1}{\triangle t}(\mathscr{B}_I\mathscr{B}_E)^{-1}. \tag{26}$$

On the other hand, for $\|\triangle t/(2Re)\mathscr{L}\| \gg 1$, applying Taylor series expansion to the inverse of $\mathscr{A}_{\mathscr{P}}$ matrix for a low Reynolds number case with sufficiently large $\triangle t$ yields to

$$\mathscr{A}_{\mathscr{P}}^{-1} \approx -2Re\mathscr{L}^{-1}. \tag{27}$$

Rather than directly calculating $\mathscr{L}^{-1}$, a further approximation for efficient computation of $\mathscr{A}_{\mathscr{P}}^{-1}$ was applied such that $\mathscr{L}^{-1} \approx -C_{\mathscr{P}}h^2\mathscr{I}_{N_E}$, where the pre-conditioning parameter $C_{\mathscr{P}}$ is a positive constant and represents a characteristic of the pre-conditioning matrix $\mathscr{P}$. Since it is non-trivial to obtain the optimal value of $C_{\mathscr{P}}$ by solving the above optimization problem, we found the optimal value of $C_{\mathscr{P}}$ through numerical simulations. The corresponding pre-conditioner matrix $\mathscr{P}$ can be defined as,

$$\mathscr{P} = \left(\mathscr{B}_I\mathscr{A}_{\mathscr{P}}^{-1}\mathscr{B}_E\right)^{-1} \approx \frac{1}{2Reh^2C_{\mathscr{P}}}(\mathscr{B}_I\mathscr{B}_E)^{-1}. \tag{28}$$

Based on $\mathscr{P}$ for the two limiting cases in Eqs. (26) and (28), the final form of $\mathscr{P}$ is expressed as,

$$\mathscr{P} = \frac{1}{\triangle t}\left(1 + \frac{\gamma}{C_{\mathscr{P}}}\right)(\mathscr{B}_I\mathscr{B}_E)^{-1} \tag{29}$$

where the diffusion parameter is defined as $\gamma = \triangle t/(2Reh^2)$.

Computational procedure Based on the choice of an appropriate pre-conditioner $\mathscr{P}$ in the previous section, we recast Eq.(21) as

$$\mathscr{B}_I\mathscr{B}_E \triangle \mathbf{F} = \left(1+\frac{\gamma}{C_{\mathscr{P}}}\right)\frac{\mathbf{U_d}-\mathscr{B}_I\mathbf{u}^{*,k-1}}{\triangle t}, \qquad (30)$$

where the dimension of $\mathscr{B}_I\mathscr{B}_E$ is $N_L \times N_L$. Note that $C_{\mathscr{P}}$ is a positive constant and represents a characteristic of the pre-conditioning matrix $\mathscr{P}$. Using the discrete delta function in Eq.(10), each component of $\mathscr{B}_I\mathscr{B}_E$ matrix is expressed as

$$(\mathscr{B}_I\mathscr{B}_E)_{ij} = \sum_E \delta_h(x_E - X_i)\delta_h(x_E - X_j)h^3 \triangle V_L, \qquad (31)$$

where the subscripts i and j indicate the column and row of the matrix, respectively. Since $\mathscr{B}_I\mathscr{B}_E$ is diagonal dominant and symmetric matrix, we use the conjugate gradient (CG) method for obtaining $\triangle\mathbf{F}$ from Eq.(31).

Details for overall procedure of the pre-conditioned IDF are summarized as follows: First, we obtain the intermediate velocity $\mathbf{u}^{*,0}$ by solving the momentum equation without forcing in Eq.(15). Next, during the IDF iterative procedure, the increment of the IB forcing $\triangle\mathbf{F}$ is obtained by solving Eq.(30) at each iteration step. Here we use CG method in the solution procedure since $\mathscr{B}_I\mathscr{B}_E$ is a positive definite. It is worthy to note that the computational time for the solution procedure might be ignorable compared to that for solving momentum equations or Poisson equation with N_E since a complexity for CG method for solving Eq.(30) is known as $\mathscr{O}(N_L)$ and N_L is typically much smaller than N_E. Moreover, it is found that a converged solution of $\triangle\mathbf{F}$ is obtained with a few iteration steps (less than 10 iterations) in CG method, because $\mathscr{B}_I\mathscr{B}_E$ is a diagonal dominant, sparse, symmetric and compact matrix. Once the intermediate velocity $\mathbf{u}^*$ converges, the Poisson equation in Eq. (4) is solved for pressure difference δp. Velocity field $\mathbf{u}^{n+1}$ at the next time step is updated by projecting the intermediate velocity to a divergence-free vector field with the pressure gradient as in Eq. (5). Also, the pressure $p^{n+1/2}$ at the next time step is updated by Eq. (6).

Theoretical comparison of DF schemes

Direct forcing

Based on the direct forcing (DF) procedure in Uhlmann (2005), IB forcing $\mathbf{F}$ is explicitly defined as,

$$\mathbf{F} = \frac{\mathbf{U_d}-\mathscr{B}_I\mathbf{u}^{*,\mathbf{0}}}{\triangle t}, \qquad (32)$$

where the forcing is proportional to the difference between the intermediate velocity and the desired velocity at the IB surface. Due to the simplicity, the DF scheme has been widely used in simulations of fluid-solid interaction problems, especially for the particle-laden flows (Lucci *et al.*, 2010). However, we found that the DF scheme may not be appropriate in providing accurate no-slip boundary conditions at the IB surface with a larger $\triangle t$ under a CFL restriction for a low Reynolds number flow. Details of numerical simulation results will be discussed later.

Within the present IDF procedure, the DF scheme in Eq. (32) can be easily derived from Eq. (16) under the assumptions of $\mathscr{A}^{-1} = \triangle t\mathscr{I}_{N_E}$ and $\mathscr{B}_I\mathscr{B}_E = \mathscr{I}_{N_E}$. The first assumption can be interpreted as the fact that the influence of convection and diffusion flow characteristics near the IB surface is ignored in the calculation of the IB forcing. This assumption is valid for a sufficiently small $\triangle t$ at moderate Reynolds number flows, while it causes numerical errors in imposing no-slip boundary conditions at the IB surface for a large $\triangle t$ or low Reynolds number flows. The second assumption indicates that each Lagrangian point has a corresponding point in the set of Eulerian grid points. This may lead to a first-order approximation of the interpolation or extrapolation for transferring velocity and IB forcing information in between Eulerian and Lagrangian points because points on the IB surface are not mostly coincided with Eulerian grid points.

Later, Su *et al.* (2007) proposed a variant of the DF scheme based on an implicit treatment of $\mathbf{F}$ with the interpolation and extrapolation operator matrices as follows:

$$\mathscr{B}_I\mathscr{B}_E\mathbf{F} = \frac{\mathbf{U_d}-\mathscr{B}_I\mathbf{u}^{*,0}}{\triangle t}, \qquad (33)$$

which can be derived from Eq. (16) with the only assumption of $\mathscr{A}^{-1} = \triangle t\mathscr{I}_{N_E}$. This scheme requires an iterative procedure such as CG method for obtaining $\mathbf{F}$ at each time step. Although the improved scheme can provide more accurate no-slip boundary conditions than the DF scheme in Eq. (32), it is found that the scheme has non-negligible numerical errors in imposing no-slip boundary conditions at the IB surface for low Reynolds number flows due to the assumption of $\mathscr{A}^{-1} = \triangle t\mathscr{I}_{N_E}$.

Multi-direct forcing

Recently, Wang *et al.* (2008) and Kempe & Fröhlich (2012) proposed a multi-direct forcing (MDF) scheme that determines $\mathbf{F}$ iteratively with the following two steps:

$$\triangle\mathbf{F} = \frac{\mathbf{U_d}-\mathscr{B}_I\mathbf{u}^{*,k-1}}{\triangle t}, \qquad (34)$$

$$\mathbf{u}^{*,k} = \mathbf{u}^{*,k-1} + \triangle t\mathscr{B}_E \triangle\mathbf{F}, \qquad (35)$$

where k denotes an iteration number for the MDF scheme. It is worthy to note that the intermediate velocity $\mathbf{u}^{*,k}$ near the IB surface is only updated by using $\triangle\mathbf{F}$ after $\mathbf{u}^{*,0}$ is obtained from the Eq. (15). Based on the present IDF procedure, it is obvious that Eq. (34) can be derived by setting the pre-conditioner matrix with $\mathscr{P} = (1/\triangle t)\mathscr{I}_{N_L}$ in Eq. (22). Also, assuming $\mathscr{A}^{-1} = \triangle t\mathscr{I}_{N_E}$ in Eq. (23) with the definition of $\triangle\mathbf{F}$ yields to the recurrence formulation of $\mathbf{u}^{*,k}$ in Eq. (35). On the other hand, $\mathbf{F}$ in Eq. (19) with $\mathscr{A}^{-1} = \triangle t\mathscr{I}_{N_E}$ and $\mathscr{P} = (1/\triangle t)\mathscr{I}_{N_L}$ can be expressed as Eq. (33). This implies that the MDF scheme is equivalent to the improved DF scheme in Su *et al.* (2007) when $\mathbf{F}$ in the MDF scheme converges. Compared to the improved DF scheme, the MDF scheme is simpler and requires no additional computational cost in constructing $\mathscr{B}_I\mathscr{B}_E$ matrix and obtaining the inverse of $\mathscr{B}_I\mathscr{B}_E$. However, the MDF also uses the assumption of $\mathscr{A}^{-1} = \triangle t\mathscr{I}_{N_E}$, which may not provide accurate no-slip boundary conditions at the IB surface for low Reynolds number flows.

Table 1. Drag and lift coefficients, and Strouhal number for flow over a circular cylinder.

	$Re = 1$	$Re = 40$	$Re = 200$		
	C_D	C_D	C_D	C_L	St
Choi *et al.* (2007)	-	1.52	1.36±0.048	±0.64	0.191
Rosenfeld *et al.* (1991)	-	-	1.31±0.04	±0.65	0.20
Tritton (1959)	11.70	1.48	-	-	-
Present IDF	12.00	1.54	1.35±0.046	±0.65	0.192

Numerical validations

Flow over a circular cylinder We consider two-dimensional flows around a fixed circular cylinder at low to moderate Reynolds number ($Re = U_\infty D/\nu$) based on the free stream velocity U_∞ and diameter of the cylinder D. The size of computational domain is $40D \times 40D$. A Dirichlet boundary condition($u/U_\infty = 1, v/U_\infty = 0$) is applied at the inflow boundary, a Neumann condition ($\partial u/\partial y = 0$) with $v = 0$ is applied at far-field boundaries, and a convective boundary condition is imposed at the outflow boundary.

To validate the present IDF method for two-dimensional flow over a bluff object, a comparison study on aerodynamic characteristics of wake flows behind the circular cylinder is performed at different Reynolds numbers. A non-uniform grid with 161×161 grid points is used in the whole domain while a uniform grid with 41×41 is used in the vicinity of the cylinder ($D \times D$) and the computational time step is determined by CFL=1.0. The pre-conditioning parameter is numerically optimized as $C_{\mathscr{P}} = 50$. Table 1 presents results for drag (C_D), lift (C_L) coefficients and strouhal number (St). Here drag and lift forces are calculated by integrating each component of IB forces at Lagrangian points (Lai & Peskin, 2000). Compared to other results from the references (Choi *et al.*, 2007; Rosenfeld *et al.*, 1991; Tritton, 1959), the present IDF method accurately predicts C_D at low Reynolds numbers ($Re = 1$ and 40) as well as unsteady characteristics such as shedding frequency and oscillations of C_D and C_L for a moderate Reynolds number ($Re = 200$).

Computational performance analysis

Numerical comparison of DF schemes Numerical simulations of two-dimensional flows over the circular cylinder for different Reynolds numbers are performed based on IB methods with different direct forcing schemes. To evaluate numerical accuracy for the different forcing schemes in imposing no-slip boundary conditions on the IB surface, the velocity error is calculated as

$$\| \triangle \mathbf{U}_e^{n+1} \|_\Gamma = \| (\mathbf{U_d} - \mathscr{B}_I \mathbf{u}^{n+1}) / U_\infty \|_\Gamma. \qquad (36)$$

Note that the computational time step is fixed with the unity of CFL number. We consider ten iterations ($N_k = 10$) per the time step for both the MDF and IDF schemes. Table 2 shows that the present IDF scheme is the most accurate among the schemes for all of Reynolds numbers. This is related to the fact that both of DF and MDF schemes use the assumption of $\mathscr{A}^{-1} = \triangle t \mathscr{I}_{N_E}$ in the calculating the IB forcing. Moreover, the velocity errors in DF scheme is larger than those in MDF scheme, which is caused by the assumption of $\mathscr{B}_I \mathscr{B}_E = \mathscr{I}_{N_E}$ in DF scheme. To visualize whether the no-slip boundary conditions are properly imposed on the IB surface, stream tracers around the circular cylinder for $Re = 1$ with CFL= 0.1 are shown in Fig. 2. This confirms that the present IDF method accurately predicts velocity fields near the IB surface not allowing the streamline to be penetrated into the immersed body.

Table 2. Velocity error $\| \triangle \mathbf{U}_e^{n+1} \|_\Gamma$ at the IB surface depending on Reynolds number for CFL= 1.

	$Re = 1$	$Re = 40$	$Re = 200$
DF	6.74×10^{-1}	1.94×10^{-1}	1.36×10^{-1}
MDF	4.82×10^{-1}	5.15×10^{-2}	1.90×10^{-2}
IDF	3.63×10^{-2}	3.64×10^{-4}	7.15×10^{-4}

Conclusion

We developed a new formulation of immersed boundary (IB) method based on direct forcing for incompressible viscous flows. The new algorithm for the present IB method were derived using block LU decomposition and Taylor series expansion, and the direct forcing for imposing no-slip condition on the IB surface was calculated in iterative procedure. We performed simulations of two-dimensional flows around a circular cylinder for low and moderate Reynolds numbers. The result showed that present IDF scheme yield a better imposition of no-slip condition on IB surface for low Reynolds number with a fairly large time step than the other direct forcing schemes.

Acknowledgment

This work is supported by the National Research Foundation of Korea(NRF) grant funded by the Korea government(MSIP) (No.NRF-2014R1A2A1A11053140 and No.2011-0029561).

REFERENCES

Choi, Jung-Il, Oberoi, Roshan C, Edwards, Jack R & Rosati, Jacky A 2007 An immersed boundary method for complex incompressible flows. *Journal of Computational Physics* **224** (2), 757–784.

Fadlun, EA, Verzicco, R, Orlandi, P_ & Mohd-Yusof, J 2000 Combined immersed-boundary finite-difference

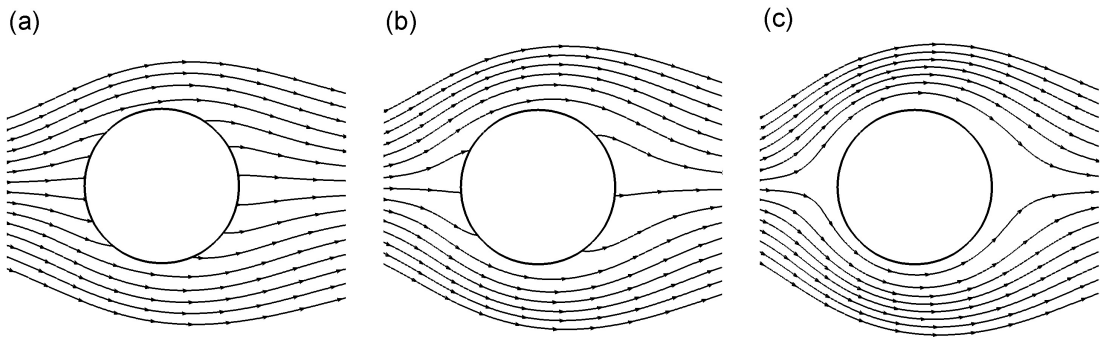

Figure 2. Stream tracers around a circular cylinder at $Re = 1$ for different direct forcing schemes; (a) DF, (b) MDF, and (c) IDF.

methods for three-dimensional complex flow simulations. *Journal of Computational Physics* **161** (1), 35–60.

Kempe, Tobias & Fröhlich, Jochen 2012 An improved immersed boundary method with direct forcing for the simulation of particle laden flows. *Journal of Computational Physics* **231** (9), 3663–3684.

Kim, Kyoungyoun, Baek, Seung-Jin & Sung, Hyung Jin 2002 An implicit velocity decoupling procedure for the incompressible navier–stokes equations. *International journal for numerical methods in fluids* **38** (2), 125–138.

Lai, Ming-Chih & Peskin, Charles S 2000 An immersed boundary method with formal second-order accuracy and reduced numerical viscosity. *Journal of Computational Physics* **160** (2), 705–719.

Lucci, Francesco, Ferrante, Antonino & Elghobashi, Said 2010 Modulation of isotropic turbulence by particles of taylor length-scale size. *Journal of Fluid Mechanics* **650**, 5–55.

Peskin, Charles S 1977 Numerical analysis of blood flow in the heart. *Journal of Computational Physics* **25** (3), 220–252.

Roma, Alexandre M, Peskin, Charles S & Berger, Marsha J 1999 An adaptive version of the immersed boundary method. *Journal of computational physics* **153** (2), 509–534.

Rosenfeld, Moshe, Kwak, Dochan & Vinokur, Marcel 1991 A fractional step solution method for the unsteady incompressible navier-stokes equations in generalized coordinate systems. *Journal of Computational Physics* **94** (1), 102–137.

Su, Shen-Wei, Lai, Ming-Chih & Lin, Chao-An 2007 An immersed boundary technique for simulating complex flows with rigid boundary. *Computers & fluids* **36** (2), 313–324.

Tritton, D.J 1959 Experiments on the flow past a circular cylinder at low reynolds numbers. *Journal of Fluid Mechanics* **6** (04), 547–567.

Uhlmann, Markus 2005 An immersed boundary method with direct forcing for the simulation of particulate flows. *Journal of Computational Physics* **209** (2), 448–476.

Wang, Zeli, Fan, Jianren & Luo, Kun 2008 Combined multi-direct forcing and immersed boundary method for simulating flows with moving particles. *International Journal of Multiphase Flow* **34** (3), 283–302.